Chapter 6

A high-order fully discrete method for two-dimensional time-fractional convection-diffusion equations with non-smooth solutions

In this chapter, we direct our focus towards the following two-dimensional time-fractional convection-diffusion equation (TFCDE)

$$ {}_{0}^{C}D_{t}^{\alpha}u = \lambda_1 u_{xx} + \lambda_2 u_{yy} + \mu_1 u_x + \mu_2 u_y + \gamma u + f, \quad \text{in } \Omega \times (0, T_f], \ \Omega \subset \mathbb{R}^2, \tag{6.1} $$

with initial and boundary conditions

$$ \begin{cases} u(x, y, 0) = \phi(x, y), & (x, y) \in \bar{\Omega} = \Omega \cup \partial\Omega, \\ u(x, y, t) = \psi(x, y, t), & (x, y) \in \partial\Omega, \ 0 < t \leq T_f, \end{cases} \tag{6.2} $$

where $\partial\Omega$ denotes the boundary of $\Omega = (0, L) \times (0, L)$, and ${}_{0}^{C}D_{t}^{\alpha}$ denotes the Caputo derivative of fractional order $\alpha \in (0, 1)$ defined in equation (1.14). Also, λ_1 and λ_2 are positive constants, and μ_1, μ_2, and γ are constants such that $\frac{\mu_1^2}{4\lambda_1} + \frac{\mu_2^2}{4\lambda_2} - \gamma \geq 0$. Further f, ϕ, and ψ are sufficiently smooth functions in their respective domains.

It is widely recognized that a typical solution to equation (6.1)-(6.2) exhibits a singularity in proximity to the initial time $t = 0$. Additionally, its derivatives meet the following regularity conditions given by [103]:

$$\left|\frac{\partial^l u}{\partial x^l}\right| \leq c, \text{ for } 0 \leq l \leq 6, \tag{6.3}$$

$$\left|\frac{\partial^l u}{\partial y^l}\right| \leq c, \text{ for } 0 \leq l \leq 6, \tag{6.4}$$

$$\left|\frac{\partial^l u}{\partial t^l}\right| \leq c(1+t^{\alpha-l}), \text{ for } 0 \leq l \leq 3, \tag{6.5}$$

where constant c is positive that does not depend on both time (t) and spatial (x, y) variables. The expression given by equation (6.5) suggests that $u(x, y, t)$ exhibits a weak singularity at $t = 0$, resulting in the time derivative $\left|\frac{\partial u}{\partial t}\right|$ becoming unbounded as $t \to 0^+$. The presence of weak initial singularity poses substantial challenges, both in practical and theoretical aspects for traditional numerical techniques due to their inability to accurately capture the behavior of the solution in the vicinity of singular points. Therefore, devising efficient numerical methods that effectively address the singularity at $t = 0$ emerges as a captivating and challenging endeavor.

In light of these considerations, the primary objective of this chapter is to develop and analyze a high-order fully discrete method for the two-dimensional TFCDE, particularly when confronted with weak initial singularities. The proposed numerical approach combines Alikhanov's high-order scheme (L2-1_σ) for the discretization of the Caputo time-fractional derivative on a non-uniform fitted mesh, along with a high-order two-dimensional compact difference operator on a uniform mesh for spatial discretization. The resulting system is solved using a robust two-step Alternating Direction Implicit (ADI) approach. The comprehensive theoretical analysis, focusing on convergence and stability, is rigorously performed using the widely recognized Fourier analysis method.

The remaining chapter follows a structured approach, beginning with the development of the numerical method for the two-dimensional TFCDE in Section 6.1. The subsequent section, Section 6.2, focuses on the stability and convergence analysis of the method. To assess its performance, numerical results are provided in Section 6.3, demonstrating the method's efficiency and accuracy. The final section, Section 6.4, concludes the chapter by summarizing the key findings.

6.1 A high-order fully discrete numerical scheme

The following section introduces a novel high-order numerical technique for solving the two-dimensional TFCDE (6.1)-(6.2). To uphold fourth-order accuracy in space and the tridiagonal property of the method, we introduce a transformation as a prerequisite to eliminate the convection terms in the equation. Notably, this transformation is similar to the one detailed in [121]. Let

$$u(x,y,t) = \frac{v(x,y,t)}{\mathcal{P}(x)\mathcal{Q}(y)}, \tag{6.6}$$

where $\mathcal{P}(x) = \exp\left(\frac{\mu_1}{2\lambda_1}x\right)$ and $\mathcal{Q}(y) = \exp\left(\frac{\mu_2}{2\lambda_2}y\right)$.

By using equations (6.1)-(6.2) and (6.6), we derive the subsequent time-fractional problem, wherein $v = v(x,y,t)$ serves as the solution:

$${}_0^C D_t^\alpha v = \lambda_1 v_{xx} + \lambda_2 v_{yy} - \mu_r v + F, \quad \text{in } \Omega \times (0, T_f],\ \Omega \subset \mathbb{R}^2, \tag{6.7}$$

with initial and boundary conditions

$$\begin{cases} v(x,y,0) = \tilde{\phi}(x,y), & (x,y) \in \bar{\Omega} = \Omega \cup \partial\Omega, \\ v(x,y,t) = \tilde{\psi}(x,y,t), & (x,y) \in \partial\Omega,\ 0 < t \leq T_f, \end{cases} \tag{6.8}$$

where $\mu_r = \frac{\mu_1^2}{4\lambda_1} + \frac{\mu_2^2}{4\lambda_2} - \gamma$, $F = \mathcal{P}(x)\mathcal{Q}(y)f$, $\tilde{\phi} = \mathcal{P}(x)\mathcal{Q}(y)\phi$, and $\tilde{\psi} = \mathcal{P}(x)\mathcal{Q}(y)\psi$.

Here, the direct implication is evident: $u(x, y, t)$ is a solution of (6.1)-(6.2) if and only if $v(x, y, t) = \mathcal{P}(x)\mathcal{Q}(y)u(x, y, t)$ is a solution of (6.7)-(6.8). Further, the subsequent step entails a detailed examination solely focused on problem (6.7)-(6.8).

6.1.1 High-order discretization of time-fractional derivative

Suppose N_t and $\hat{N}_t$ are positive integers, satisfying the conditions $\hat{N}_t \leq N_t$ and $\hat{N}_t \geq cN_t$, where c is a fixed constant in $(0, 1)$. We partition the interval $[0, T_f]$ into two subintervals $[0, T]$ and $[T, T_f]$, where $T \in (0, T_f]$ is arbitrary. To divide $[0, T]$, we employ a graded mesh with mesh points denoted by $t_i = T\left(\frac{i}{\hat{N}_t}\right)^{\theta}$ for $0 \leq i \leq \hat{N}_t$. The user has the flexibility to select the grading parameter θ subject to the constraint $\theta \geq 1$. Further, for ease of implementation, we consider the quasiuniform mesh on the interval $[T, T_f]$ (i.e., the ratio $\max_i \Delta t_i / \min_i \Delta t_i$ is always kept within a constant limit), with mesh points $T = t_{\hat{N}_t} < t_{\hat{N}_t+1} < \cdots < t_{N_t-1} < t_{N_t} = T_f$. The term "fitted" is used to describe this mesh because, through the proper choice of the grading parameter θ, the graded section of the mesh adeptly manages functions with a weak singularity at $t = 0$.

Further, set $\Delta t_i = t_i - t_{i-1}$, for $1 \leq i \leq N_t$ and $t_{i+\sigma} = t_i + \sigma\Delta t_{i+1}$, for $0 \leq i \leq N_t - 1$. By employing Alikhanov's formula (L2-1_σ), we approximate the Caputo derivative of function $g \in C[0, T_f] \cap C^3(0, T_f]$ at $t_{i+\sigma}$ given in [18]

$$
{}_0^C D_t^{\alpha} g(t_{i+\sigma}) = w_{i,i}^{(\alpha,\sigma)} g(t_{i+1}) - \sum_{k=1}^{i} \left(w_{i,k}^{(\alpha,\sigma)} - w_{i,k-1}^{(\alpha,\sigma)} \right) g(t_k) - w_{i,0}^{(\alpha,\sigma)} g(t_0) + (\mathcal{R}_t^{\alpha})^{i+\sigma}, \tag{6.9}
$$

where $(\mathcal{R}_t^{\alpha})^{i+\sigma}$ is the local truncation error term and the coefficients $w^{(\alpha,\sigma)}$'s are given as $w_{0,0}^{(\alpha,\sigma)} = \Delta t_1^{-1} r_{0,0}^{(\alpha,\sigma)}$, and for $i \geq 1$,

$$w_{i,k}^{(\alpha,\sigma)} = \begin{cases} \Delta t_{k+1}^{-1}\left(r_{i,0}^{(\alpha,\sigma)} + s_{i,0}^{(\alpha,\sigma)}\right), & k = 0, \\ \Delta t_{k+1}^{-1}\left(r_{i,k}^{(\alpha,\sigma)} + s_{i,k-1}^{(\alpha,\sigma)} - s_{i,k}^{(\alpha,\sigma)}\right), & 1 \leq k \leq i-1, \\ \Delta t_{k+1}^{-1}\left(r_{i,i}^{(\alpha,\sigma)} + s_{i,i-1}^{(\alpha,\sigma)}\right), & k = i, \end{cases} \tag{6.10}$$

with

$$r_{i,i}^{(\alpha,\sigma)} = \frac{\sigma^{1-\alpha}}{\Gamma(2-\alpha)} \Delta t_{i+1}^{1-\alpha}, \text{ for } i \geq 0, \tag{6.11}$$

and for $i \geq 1$, $0 \leq k \leq i-1$,

$$r_{i,k}^{(\alpha,\sigma)} = \frac{1}{\Gamma(1-\alpha)} \int_{t_k}^{t_{k+1}} (t_{i+\sigma} - \tau)^{-\alpha} d\tau, \tag{6.12}$$

$$s_{i,k}^{(\alpha,\sigma)} = \frac{1}{\Gamma(1-\alpha)} \frac{2}{(t_{k+2} - t_k)} \int_{t_k}^{t_{k+1}} (t_{i+\sigma} - \tau)^{-\alpha} (\tau - t_{k+1/2}) d\tau. \tag{6.13}$$

Lemma 6.1. [18] *Suppose* $1 - \alpha/2 \leq \sigma \leq 1$ *and the local mesh ratio* $\eta_i = \frac{\Delta t_{i+1}}{\Delta t_i}$ *for* $1 \leq i \leq N_t - 1$ *satisfies* $3/4 \leq \eta_i \leq 62$*. Then*

(i). $w_{i,0}^{(\alpha,\sigma)} > \dfrac{t_{i+\sigma}^{-\alpha}}{\Gamma(1-\alpha)} > 0, \ i \geq 0.$

(ii). $(2\sigma - 1) w_{1,1}^{(\alpha,\sigma)} - \sigma w_{1,0}^{(\alpha,\sigma)} > 0.$

(iii). $w_{i,1}^{(\alpha,\sigma)} > w_{i,0}^{(\alpha,\sigma)}, \quad i \geq 1.$

(iv). *If* $\eta_{k-1}^2(\eta_{k-1} + 1) \geq \dfrac{\eta_k}{\eta_k + 1}$ *for* $2 \leq k \leq i$, *with* $i \geq 2$, *then* $w_{i,k-1}^{(\alpha,\sigma)} < w_{i,k}^{(\alpha,\sigma)}$.

(v). *If* $\eta_{i-1}^2\left(2 - \dfrac{1}{\sigma} + \eta_i(\eta_i + 2)\right) \geq \dfrac{\eta_i(\eta_i + 1)}{\eta_{i-1} + 1}$ *for* $2 \leq i \leq N_t$, *then*

$$(2\sigma - 1) w_{i,i}^{(\alpha,\sigma)} - \sigma w_{i,i-1}^{(\alpha,\sigma)} > 0.$$

At point $t = t_{i+\sigma}$, equation (6.7) takes the form

$$ {}_0^C D_t^{\alpha} v^{i+\sigma}(x,y) = \lambda_1 v_{xx}^{i+\sigma}(x,y) + \lambda_2 v_{yy}^{i+\sigma}(x,y) - \mu_r v^{i+\sigma}(x,y) + F^{i+\sigma}(x,y), $$
$$ (x,y) \in \Omega,\ 0 \leq i \leq N_t - 1, \tag{6.14} $$

with initial and boundary conditions

$$ \begin{cases} u^0(x,y) = \tilde{\phi}(x,y), & (x,y) \in \bar{\Omega} = \Omega \cup \partial\Omega, \\ u^i(x,y) = \tilde{\psi}(x,y,t_i), & (x,y) \in \partial\Omega,\ 1 \leq i \leq N_t, \end{cases} \tag{6.15} $$

where we denote $u^i(x,y) = u(x,y,t_i)$. Employing the L2-1_σ approximation on a non-uniform mesh, as described in equation (6.9), and incorporating it into equation (6.14), yields the following semi-discrete scheme

$$ w_{i,i}^{(\alpha,\sigma)} v^{i+1}(x,y) - \sum_{k=1}^{i} \left(w_{i,k}^{(\alpha,\sigma)} - w_{i,k-1}^{(\alpha,\sigma)} \right) v^k(x,y) - w_{i,0}^{(\alpha,\sigma)} v^0(x,y) + (\mathcal{R}_t^{\alpha})^{i+\sigma} = \lambda_1 \times $$
$$ v_{xx}^{i+\sigma}(x,y) + \lambda_2 v_{yy}^{i+\sigma}(x,y) - \mu_r v^{i+\sigma}(x,y) + F^{i+\sigma}(x,y),\ (x,y) =: \Omega,\ 0 \leq i \leq N_t - 1. \tag{6.16} $$

6.1.2 High-order compact alternating direction implicit (ADI) scheme

Now, our subsequent strategy for solving the two-dimensional problem (6.16) with initial and boundary conditions (6.15) entails the discretization of the spatial variables through the utilization of a compact finite difference scheme. The compact finite difference method is a well-established numerical technique extensively utilized in solving PDEs. It has been studied and applied in various scientific and engineering fields. Numerous research works have demonstrated the effectiveness and advantages of the high-order compact finite difference method [30, 58, 71, 100, 104]. For given positive integers N_x and N_y, we discretize the problem using $x_m = mh_x$ and $y_n = nh_y$, where $0 \leq m \leq N_x$ and $0 \leq n \leq N_y$. Here, $h_x = \frac{L}{N_x}$ is the step size in the x direction, and $h_y = \frac{L}{N_y}$ is the step size in the y direction. Let $v = \{v^i_{m,n} \mid 0 \leq m \leq N_x, 0 \leq n \leq N_y, \text{ and } 1 \leq i \leq N_t\}$. We introduce spatial difference operators

$$\mathcal{H}_x v^i_{m,n} = \begin{cases} \left(I + \frac{h_x^2}{12}\delta_x^2\right) v^i_{m,n}, & 1 \leq m \leq M_x - 1, \\ v^i_{m,n}, & m = 0 \text{ or } M_x, \end{cases} \tag{6.17}$$

$$\mathcal{H}_y v^i_{m,n} = \begin{cases} \left(I + \frac{h_y^2}{12}\delta_y^2\right) v^i_{m,n}, & 1 \leq n \leq M_y - 1, \\ v^i_{m,n}, & n = 0 \text{ or } M_y, \end{cases} \tag{6.18}$$

where

$$\delta_x^2 v^i_{m,n} = \frac{v^i_{m+1,n} - 2v^i_{m,n} + v^i_{m-1,n}}{h_x^2} \quad \text{and} \quad \delta_y^2 v^i_{m,n} = \frac{v^i_{m,n+1} - 2v^i_{m,n} + v^i_{m,n-1}}{h_y^2}. \tag{6.19}$$

Now, re-write equation (6.16) at (x_m, y_n) in the following form

$$-\lambda_1 v^{i+\sigma}_{xx}(x_m, y_n) - \lambda_2 v^{i+\sigma}_{yy}(x_m, y_n) = G^{i+\sigma}(x_m, y_n) + (\mathcal{R}^\alpha_t)^{i+\sigma}, \tag{6.20}$$

where

$$\begin{aligned} G^{i+\sigma}(x_m, y_n) = F^{i+\sigma}(x_m, y_n) - w^{(\alpha,\sigma)}_{i,i} v^{i+1}(x_m, y_n) + \sum_{k=1}^{i} \left(w^{(\alpha,\sigma)}_{i,k} - w^{(\alpha,\sigma)}_{i,k-1}\right) v^k(x_m, y_n) \\ + w^{(\alpha,\sigma)}_{i,0} v^0(x_m, y_n) - \mu_r v^{i+\sigma}(x_m, y_n). \end{aligned} \tag{6.21}$$

In accordance with the techniques presented in [70, 124], we develop a fourth-order compact scheme for equation (6.20) as follows

$$-\lambda_1 \mathcal{H}_x^{-1}\delta_x^2 v_{m,n}^{i+\sigma} - \lambda_2 \mathcal{H}_y^{-1}\delta_y^2 v_{m,n}^{i+\sigma} = G_{m,n}^{i+\sigma} + (\mathcal{R}_t^{\alpha})^{i+\sigma} + (\mathcal{R}_l)_{m,n}^{i+\sigma}, \tag{6.22}$$

where

$$(\mathcal{R}_l)_{m,n}^{i+\sigma} = (\mathcal{R}_x)_{m,n}^{i+\sigma} + (\mathcal{R}_y)_{m,n}^{i+\sigma},$$

with $\varphi(\upsilon) = -3(1-\upsilon)^5 + 5(1-\upsilon)^3$, and

$$(\mathcal{R}_x)_{m,n}^{i+\sigma} = \frac{h_x^4}{360}\int_0^1 \left(\frac{\partial^6 v}{\partial x^6}(x_m - \upsilon h_x, y_n, t_{i+\sigma}) + \frac{\partial^6 v}{\partial x^6}(x_m + \upsilon h_x, y_n, t_{i+\sigma})\right)\varphi(\upsilon)d\upsilon,$$
$$(\mathcal{R}_y)_{m,n}^{i+\sigma} = \frac{h_y^4}{360}\int_0^1 \left(\frac{\partial^6 v}{\partial y^6}(x_m, y_n - \upsilon h_y, t_{i+\sigma}) + \frac{\partial^6 v}{\partial y^6}(x_m, y_n + \upsilon h_y, t_{i+\sigma})\right)\varphi(\upsilon)d\upsilon.$$

Thus, we have

$$(\mathcal{R}_l)_{m,n}^{i+\sigma} \leq c\ (h_x^4 + h_y^4). \tag{6.23}$$

By multiplying both sides of equation (6.22) with the operator $\mathcal{H}_x\mathcal{H}_y$, we obtain

$$(-\lambda_1 \mathcal{H}_y\delta_x^2 - \lambda_2 \mathcal{H}_x\delta_y^2)v_{m,n}^{i+\sigma} = \mathcal{H}_x\mathcal{H}_y G_{m,n}^{i+\sigma} + (\mathcal{R}_t^{\alpha})^{i+\sigma} + (\mathcal{R}_l)_{m,n}^{i+\sigma}. \tag{6.24}$$

Lemma 6.2. [18] *For any function $g(t) \in C^2(0, T_f]$, one has*

$$|g(t_{i+\sigma}) - \{\sigma g(t_{i+1}) + (1-\sigma)g(t_i)\}| \leq \frac{\Delta t_{i+1}^2}{8}\max_{1\leq i\leq N_t}|g''(t_i)|.$$

Therefore, by utilizing Lemma 6.2 along with equation (6.21), into equation (6.24), we obtain the following expression

$$\nu\left(\mathcal{H}_x\mathcal{H}_y - \frac{\sigma\lambda_1}{\nu}\mathcal{H}_y\delta_x^2 - \frac{\sigma\lambda_2}{\nu}\mathcal{H}_x\delta_y^2\right)v_{m,n}^{i+1} = \sum_{k=1}^{i}\left(w_{i,k}^{(\alpha,\sigma)} - w_{i,k-1}^{(\alpha,\sigma)}\right)\mathcal{H}_x\mathcal{H}_y v_{m,n}^k + w_{i,0}^{(\alpha,\sigma)}$$
$$\times \mathcal{H}_x\mathcal{H}_y v_{m,n}^0 - \mu_r(1-\sigma)\mathcal{H}_x\mathcal{H}_y v_{m,n}^i + (1-\sigma)(\lambda_1\mathcal{H}_y\delta_x^2 + \lambda_2\mathcal{H}_x\delta_y^2)v_{m,n}^i + \mathcal{H}_x\mathcal{H}_y F_{m,n}^{i+\sigma}$$
$$+ (\mathcal{R}_t^{\alpha})^{i+\sigma} + (\mathcal{R}_l)_{m,n}^{i+\sigma} + \mathcal{R}_t^{i+1},$$

where, $\nu = \mu_r\sigma + w_{i,i}^{(\alpha,\sigma)} > 0$. Also, by invoking Lemma 6.2, we can obtain a bound for $\mathcal{R}_t^{i+1}$. After re-arranging the terms of above equation, we get

$$\left(\mathcal{H}_x\mathcal{H}_y - \frac{\sigma\lambda_1}{\nu}\mathcal{H}_y\delta_x^2 - \frac{\sigma\lambda_2}{\nu}\mathcal{H}_x\delta_y^2\right)v_{m,n}^{i+1} = \frac{1}{\nu}\sum_{k=1}^{i}\left(w_{i,k}^{(\alpha,\sigma)} - w_{i,k-1}^{(\alpha,\sigma)}\right)\mathcal{H}_x\mathcal{H}_y v_{m,n}^k$$
$$+ \frac{w_{i,0}^{(\alpha,\sigma)}}{\nu}\mathcal{H}_x\mathcal{H}_y v_{m,n}^0 - \frac{\mu_r(1-\sigma)}{\nu}\mathcal{H}_x\mathcal{H}_y v_{m,n}^i + \frac{(1-\sigma)}{\nu}\left(\lambda_1\mathcal{H}_y\delta_x^2 + \lambda_2\mathcal{H}_x\delta_y^2\right)v_{m,n}^i$$
$$+ \frac{1}{\nu}\mathcal{H}_x\mathcal{H}_y F_{m,n}^{i+\sigma} + \frac{(\mathcal{R}_t^{\alpha})^{i+\sigma}}{\nu} + \frac{(\mathcal{R}_l)_{m,n}^{i+\sigma}}{\nu} + \frac{\mathcal{R}_t^{i+1}}{\nu}. \tag{6.25}$$

Further, to devise an efficient ADI scheme, we incorporate the following perturbation term

$$\frac{\lambda_1\lambda_2\sigma^2}{\nu^2}\delta_x^2\delta_y^2(v_{m,n}^{i+1} - v_{m,n}^i) = (\mathcal{R}_p)_{m,n}^{i+1}. \tag{6.26}$$

Now, adding this perturbation term in equation (6.25), we get

$$\left(\mathcal{H}_x - \frac{\sigma\lambda_1}{\nu}\delta_x^2\right)\left(\mathcal{H}_y - \frac{\sigma\lambda_2}{\nu}\delta_y^2\right)v_{m,n}^{i+1} = \frac{1}{\nu}\sum_{k=1}^{i}\left(w_{i,k}^{(\alpha,\sigma)} - w_{i,k-1}^{(\alpha,\sigma)}\right)\mathcal{H}_x\mathcal{H}_y v_{m,n}^k$$
$$+ \frac{w_{i,0}^{(\alpha,\sigma)}}{\nu}\mathcal{H}_x\mathcal{H}_y v_{m,n}^0 - \frac{\mu_r(1-\sigma)}{\nu}\mathcal{H}_x\mathcal{H}_y v_{m,n}^i + \frac{(1-\sigma)}{\nu}\left(\lambda_1\mathcal{H}_y\delta_x^2 + \lambda_2\mathcal{H}_x\delta_y^2\right)v_{m,n}^i$$
$$+ \frac{1}{\nu}\mathcal{H}_x\mathcal{H}_y F_{m,n}^{i+\sigma} + \frac{\lambda_1\lambda_2\sigma^2}{\nu^2}\delta_x^2\delta_y^2 v_{m,n}^i + (\mathcal{R}_f)_{m,n}^{i+1}, \tag{6.27}$$

where

$$(\mathcal{R}_f)_{m,n}^{i+1} = \frac{(\mathcal{R}_t^{\alpha})^{i+\sigma}}{\nu} + \frac{(\mathcal{R}_l)_{m,n}^{i+\sigma}}{\nu} + \frac{\mathcal{R}_t^{i+1}}{\nu} + (\mathcal{R}_p)_{m,n}^{i+1}. \tag{6.28}$$

By omitting the error term in equation (6.27), we derive the following fully discrete numerical scheme

$$\begin{aligned}\left(\mathcal{H}_x - \frac{\sigma\lambda_1}{\nu}\delta_x^2\right)\left(\mathcal{H}_y - \frac{\sigma\lambda_2}{\nu}\delta_y^2\right)V_{m,n}^{i+1} &= \frac{1}{\nu}\sum_{k=1}^{i}\left(w_{i,k}^{(\alpha,\sigma)} - w_{i,k-1}^{(\alpha,\sigma)}\right)\mathcal{H}_x\mathcal{H}_y V_{m,n}^k \\ &+ \frac{w_{i,0}^{(\alpha,\sigma)}}{\nu}\mathcal{H}_x\mathcal{H}_y V_{m,n}^0 - \frac{\mu_r(1-\sigma)}{\nu}\mathcal{H}_x\mathcal{H}_y V_{m,n}^i + \frac{(1-\sigma)}{\nu}\left(\lambda_1\mathcal{H}_y\delta_x^2 + \lambda_2\mathcal{H}_x\delta_y^2\right)V_{m,n}^i \\ &+ \frac{1}{\nu}\mathcal{H}_x\mathcal{H}_y F_{m,n}^{i+\sigma} + \frac{\lambda_1\lambda_2\sigma^2}{\nu^2}\delta_x^2\delta_y^2 V_{m,n}^i,\end{aligned} \tag{6.29}$$

where $V_{m,n}^i$ represents the numerical approximation of $v_{m,n}^i$.

Further, to enhance the ease of computations, we incorporate the intermediate variable $V_{m,n}^*$ defined by

$$V_{m,n}^* = \left(\mathcal{H}_y - \frac{\sigma\lambda_2}{\nu}\delta_y^2\right)V_{m,n}^{i+1},\ 0 \le m \le N_x,\ 1 \le n \le N_y - 1. \tag{6.30}$$

Now, by employing a sequential two-step procedure, equation (6.29) can be effectively solved as described below:

Step (i): To determine $\{V_{m,n}^*\}$, we solve the following set of linear equations, for a fixed $n \in \{1, 2, \ldots N_y - 1\}$,

$$\begin{aligned}\left(\mathcal{H}_x - \frac{\sigma\lambda_1}{\nu}\delta_x^2\right)V_{m,n}^* &= \frac{1}{\nu}\sum_{k=1}^{i}\left(w_{i,k}^{(\alpha,\sigma)} - w_{i,k-1}^{(\alpha,\sigma)}\right)\mathcal{H}_x\mathcal{H}_y V_{m,n}^k + \frac{w_{i,0}^{(\alpha,\sigma)}}{\nu}\mathcal{H}_x\mathcal{H}_y V_{m,n}^0 \\ &- \frac{\mu_r(1-\sigma)}{\nu}\mathcal{H}_x\mathcal{H}_y V_{m,n}^i + \frac{(1-\sigma)}{\nu}\left(\lambda_1\mathcal{H}_y\delta_x^2 + \lambda_2\mathcal{H}_x\delta_y^2\right)V_{m,n}^i + \frac{1}{\nu}\mathcal{H}_x\mathcal{H}_y F_{m,n}^{i+\sigma} \\ &+ \frac{\lambda_1\lambda_2\sigma^2}{\nu^2}\delta_x^2\delta_y^2 V_{m,n}^i,\quad 1 \le m \le N_x - 1,\end{aligned} \tag{6.31}$$

with boundary conditions

$$V^*_{0,n} = \left(\mathcal{H}_y - \frac{\sigma\lambda_2}{\nu}\delta_y^2\right) V^{i+1}_{0,n}, \quad V^*_{N_x,n} = \left(\mathcal{H}_y - \frac{\sigma\lambda_2}{\nu}\delta_y^2\right) V^{i+1}_{N_x,n}, \tag{6.32}$$

where

$$V^{i+1}_{0,n} = \tilde{\psi}(x_0, y_n, t_{i+1}), \quad V^{i+1}_{N_x,n} = \tilde{\psi}(x_{N_x}, y_n, t_{i+1}). \tag{6.33}$$

Step (ii): Once the $\{V^*_{m,n}\}$ values have been determined, we solve the subsequent set of linear equations to obtain the final solution $\{V^{i+1}_{m,n}\}$, for a fixed $m \in \{1, 2, \ldots N_x - 1\}$, as follows

$$\left(\mathcal{H}_y - \frac{\sigma\lambda_2}{\nu}\delta_y^2\right) V^{i+1}_{m,n} = V^*_{m,n}, \quad 1 \leq n \leq N_y - 1, \tag{6.34}$$

with boundary conditions

$$V^{i+1}_{m,0} = \tilde{\psi}(x_m, y_0, t_{i+1}), \quad V^{i+1}_{m,N_y} = \tilde{\psi}(x_m, y_{N_y}, t_{i+1}). \tag{6.35}$$

6.2 Theoretical analysis

We will now explore the truncation error, stability, and convergence aspects of the developed scheme in this section.

6.2.1 Truncation error

Now, we proceed to estimate the truncation error, denoted as $(\mathcal{R}_f)^{i+1}_{m,n}$, of the scheme (6.29).

Lemma 6.3. *Let* $\sigma = 1 - \frac{\alpha}{2}$. *Assume that the local mesh ratio* $\eta_i = \frac{\Delta t_{i+1}}{\Delta t_i}$ *for* $1 \leq i \leq N_t - 1$ *satisfies* $3/4 \leq \eta_i \leq 62$. *Then*

$$\frac{1}{w_{i,i}^{(\alpha,\sigma)}} = \mathcal{O}(\Delta t_{i+1}^{\alpha}), \ \ for \ 0 \leq i \leq N_t - 1.$$

Proof. It is obvious for $i = 0$ that

$$w_{0,0}^{(\alpha,\sigma)} = \frac{\sigma^{1-\alpha}}{\Gamma(2-\alpha)} \frac{1}{\Delta t_1^{\alpha}},$$

which imply

$$\left| \frac{1}{w_{0,0}^{(\alpha,\sigma)}} \right| \leq \frac{\Gamma(2-\alpha)}{\sigma^{1-\alpha}} \Delta t_1^{\alpha}. \tag{6.36}$$

For $i \geq 1$,

$$w_{i,i}^{(\alpha,\sigma)} = \frac{1}{\Delta t_{i+1}} \left(r_{i,i}^{(\alpha,\sigma)} + s_{i,i-1}^{(\alpha,\sigma)} \right) = \frac{1}{\Delta t_{i+1}^{\alpha}} \left[\frac{\sigma^{1-\alpha}}{\Gamma(2-\alpha)} + \frac{s_{i,i-1}^{(\alpha,\sigma)}}{\Delta t_{i+1}^{1-\alpha}} \right],$$

which on solving yields

$$w_{i,i}^{(\alpha,\sigma)} = \frac{\sigma^{1-\alpha}}{\Gamma(2-\alpha)} \frac{\varrho}{\Delta t_{i+1}^{\alpha}}, \tag{6.37}$$

where

$$\varrho = 1 + \left(1 + \frac{1}{\eta_i}\right)^{-1} \left[\left\{ \left(1 + \frac{1}{\sigma \eta_i}\right)^{2-\alpha} - 1 \right\} - \frac{1}{\eta_i} \left\{ \left(1 + \frac{1}{\sigma \eta_i}\right)^{1-\alpha} + 1 \right\} \right],$$

with $\eta_i = \frac{\Delta t_{i+1}}{\Delta t_i}$. Further, by employing the bounds of η_i, where $1 \leq i \leq N_t - 1$, with values confined within the range $3/4 \leq \eta_i \leq 62$, as established in [18], we can derive the corresponding bounds of ϱ as

$$1.6597542 \leq \varrho \leq 13.215168. \tag{6.38}$$

By utilizing the relation (6.36) and incorporating the bounds of ϱ as provided in (6.38) into the expression (6.37), we obtain the following result

$$\left| \frac{1}{w_{i,i}^{(\alpha,\sigma)}} \right| \leq c\ \Delta t_{i+1}^{\alpha},$$

where c is a positive constant.

Thus, we have the Lemma. □

Now we define the following functions

$$\begin{cases} Q_g^{\sigma} & = \Delta t_1^{\alpha} \sup\limits_{\varepsilon\in(0,t_1)} \left(\varepsilon^{1-\alpha}|\delta_t g(t_0) - g'(\varepsilon)|\right), \\ Q_g^{i+\sigma} & = t_{i+\sigma}^{\alpha}\Delta t_{i+1}^{3-\alpha} \sup\limits_{\varepsilon\in(t_i,t_{i+1})} |g'''(\varepsilon)|, \text{ for } 1 \leq i \leq N_t - 1, \\ Q_g^{i,1} & = \Delta t_1^{\alpha} \sup\limits_{\varepsilon\in(0,t_1)} \left(\varepsilon^{1-\alpha}|(I_{2,1}g(\varepsilon))' - g'(\varepsilon)|\right), \text{ for } 1 \leq i \leq N_t - 1, \\ Q_g^{i,k} & = t_k^{\alpha}\Delta t_{i+1}^{-\alpha}\Delta t_k^2(\Delta t_{k+1} + \Delta t_k) \sup\limits_{\varepsilon\in(t_{k-1},t_{k+1})} |g'''(\varepsilon)|, \text{ for } 2 \leq k \leq i \leq N_t - 1, \end{cases} \tag{6.39}$$

for any function $g \in C[0,T] \cap C^3(0,T]$. Here, $\delta_t g(t_0) = \frac{[g(t_1)-g(t_0)]}{\Delta t_1}$ and $I_{2,1}g(\varepsilon)$ is the quadratic polynomial that interpolates to $g(\varepsilon)$ at the points t_0, t_1, and t_2.

Lemma 6.4. [18] *Given the assumptions $\sigma = 1 - \frac{\alpha}{2}$, $\Delta t_{i+1} \lesssim t_i$ for $i \geq 2$, and $\frac{\Delta t_1}{\Delta t_2} \leq \rho$ (with ρ being a positive constant), the following result holds true for any function $g(t) \in C^3(0,T]$:*

$$\left|(\mathcal{R}_t^{\alpha})^{i+\sigma}\right| \lesssim t_{i+\sigma}^{-\alpha} \left(Q_g^{i+\sigma} + \max_{1\leq k\leq i}\{Q_g^{i,k}\} \right), \ \textit{for } 0 \leq i \leq N_t - 1.$$

Lemma 6.5. [18] *Suppose* $g \in C[0,T] \cap C^3(0,T]$ *and satisfies the assumptions stated in (6.5). Then*

$$Q_g^{i+\sigma} \lesssim N_t^{-\min\{3-\alpha,\theta\alpha\}}, \ \textit{for } 0 \le i \le N_t - 1,$$
$$Q_g^{i,k} \lesssim N_t^{-\min\{3-\alpha,\theta\alpha\}}, \ \textit{for } 1 \le k \le i, \ \textit{when } i \ge 1.$$

Thus, combining Lemmas 6.4 and 6.5, we get

$$\left|(\mathcal{R}_t^{\alpha})^{i+\sigma}\right| \lesssim t_{i+\sigma}^{-\alpha} N_t^{-\min\{3-\alpha,\theta\alpha\}}, \ \text{for } 0 \le i \le N_t - 1. \tag{6.40}$$

Theorem 6.1. *Suppose that the solution* $v(x,y,t)$ *of problem (6.7)-(6.8) meets the assumptions provided in (6.3)-(6.5). Then, the local truncation error* $(\mathcal{R}_f)_{m,n}^{i+1}$*, given in equation (6.28), of the scheme (6.29) satisfies the following bound*

$$|(\mathcal{R}_f)_{m,n}^{i+1}| \le c\left(N_t^{-\min\{3-\alpha,\theta\alpha,1+2\alpha,2+\alpha\}} + h_x^4 + h_y^4\right).$$

Proof. Based on equation (6.28), and $w_{i,i}^{(\alpha,\sigma)} > 0$, we deduce that

$$\begin{aligned}|(\mathcal{R}_f)_{m,n}^{i+1}| &\le \left|\frac{(\mathcal{R}_t^{\alpha})^{i+\sigma}}{\nu}\right| + \left|\frac{(\mathcal{R}_l)_{m,n}^{i+\sigma}}{\nu}\right| + \left|\frac{\mathcal{R}_t^{i+1}}{\nu}\right| + \left|(\mathcal{R}_p)_{m,n}^{i+1}\right| \\ &\le \frac{|(\mathcal{R}_t^{\alpha})^{i+\sigma}|}{w_{i,i}^{(\alpha,\sigma)}} + \frac{|(\mathcal{R}_l)_{m,n}^{i+\sigma}|}{w_{i,i}^{(\alpha,\sigma)}} + \frac{|\mathcal{R}_t^{i+1}|}{w_{i,i}^{(\alpha,\sigma)}} + \left|(\mathcal{R}_p)_{m,n}^{i+1}\right|.\end{aligned} \tag{6.41}$$

Next, we proceed to bound each term individually in inequality (6.41).

Utilizing Lemma 6.3 together with inequality (6.40), we arrive at

$$\begin{aligned}\frac{|(\mathcal{R}_t^{\alpha})^{i+\sigma}|}{w_{i,i}^{(\alpha,\sigma)}} &\le c\ \Delta t_{i+1}^{\alpha} t_{i+\sigma}^{-\alpha} N_t^{-\min\{3-\alpha,\theta\alpha\}} \\ &= c\ \Delta t_{i+1}^{\alpha}(t_i + \sigma\Delta t_{i+1})^{-\alpha} N_t^{-\min\{3-\alpha,\theta\alpha\}}\end{aligned}$$

$$
\begin{aligned}
&\leq c\ \Delta t_{i+1}^{\alpha}(\sigma \Delta t_{i+1})^{-\alpha} N_t^{-\min\{3-\alpha,\theta\alpha\}} \\
&\leq c\ N_t^{-\min\{3-\alpha,\theta\alpha\}}.
\end{aligned} \tag{6.42}
$$

Next, we invoke Lemma 6.3 along with relation (6.25) to obtain

$$
\frac{|(\mathcal{R}_l)_{m,n}^{i+\sigma}|}{w_{i,i}^{(\alpha,\sigma)}} \leq c\ (h_x^4 + h_y^4). \tag{6.43}
$$

Moving forward, by merging Lemmas 6.2 and 6.3, we get

$$
\frac{|\mathcal{R}_t^{i+1}|}{w_{i,i}^{(\alpha,\sigma)}} \leq\ c\ \Delta t_{i+1}^{2+\alpha}. \tag{6.44}
$$

Moreover, it is evident from [103] that

$$
\Delta t_{i+1} \leq C\ T_f N_t^{-\theta} i^{\theta-1} \leq C\ T_f N_t^{-\theta} N_t^{\theta-1} \leq \frac{C\ T_f}{N_t}. \tag{6.45}
$$

Hence, by employing equations (6.44) and (6.45), we deduce that

$$
\frac{|\mathcal{R}_t^{i+1}|}{w_{i,i}^{(\alpha,\sigma)}} \leq\ c\ N_t^{-(2+\alpha)}. \tag{6.46}
$$

Finally, by combining Lemma 6.3 with equation (6.26) and incorporating relation (6.45), we obtain

$$
|(\mathcal{R}_p)_{m,n}^{i+1}| \leq\ c\ N_t^{-(1+2\alpha)}. \tag{6.47}
$$

Therefore, by substituting equations (6.42), (6.43), (6.46), and (6.47) into relation (6.41), we have the theorem. □

6.2.2 Stability analysis

Let the scheme (6.29) having a perturbed solution $\{\widetilde{V}^i_{m,n}, 1 \leq m \leq N_x-1,\ 1 \leq n \leq N_y-1,\ 1 \leq i \leq N_t\}$. Then, we will examine how the perturbation $\zeta^i_{m,n} = V^i_{m,n} - \widetilde{V}^i_{m,n}$, $1 \leq m \leq N_x-1,\ 1 \leq n \leq N_y-1,\ 1 \leq i \leq N_t$, evolves over time. Note that $\zeta^i_{m,n}$ satisfies the following error equation

$$\begin{aligned}
&\left(\mathcal{H}_x - \frac{\sigma\lambda_1}{\nu}\delta_x^2\right)\left(\mathcal{H}_y - \frac{\sigma\lambda_2}{\nu}\delta_y^2\right)\zeta^{i+1}_{m,n} = \frac{1}{\nu}\sum_{k=1}^{i}\left(w^{(\alpha,\sigma)}_{i,k} - w^{(\alpha,\sigma)}_{i,k-1}\right)\mathcal{H}_x\mathcal{H}_y\zeta^k_{m,n}\\
&+\frac{w^{(\alpha,\sigma)}_{i,0}}{\nu}\mathcal{H}_x\mathcal{H}_y\zeta^0_{m,n} - \frac{\mu_r(1-\sigma)}{\nu}\mathcal{H}_x\mathcal{H}_y\zeta^i_{m,n} + \frac{(1-\sigma)}{\nu}\left(\lambda_1\mathcal{H}_y\delta_x^2 + \lambda_2\mathcal{H}_x\delta_y^2\right)\zeta^i_{m,n}\\
&+\frac{\lambda_1\lambda_2\sigma^2}{\nu^2}\delta_x^2\delta_y^2\zeta^i_{m,n},\quad 1 \leq m \leq N_x-1,\ 1 \leq n \leq N_y-1,\ 0 \leq i \leq N_t-1,
\end{aligned} \tag{6.48}$$

where

$$\zeta^{i+1} = [\zeta^{i+1}_{1,1}, \zeta^{i+1}_{1,2}, \ldots, \zeta^{i+1}_{1,N_y-1}, \zeta^{i+1}_{2,1}, \zeta^{i+1}_{2,2}, \ldots, \zeta^{i+1}_{2,N_y-1}, \ldots, \zeta^{i+1}_{N_x-1,1}, \zeta^{i+1}_{N_x-1,2}, \ldots, \zeta^{i+1}_{N_x-1,N_y-1}]^T.$$

The grid function $\zeta^{i+1}(x,y),\ 0 \leq i \leq N_t-1$, is defined as

$$\zeta^{i+1}(x,y) = \begin{cases} \zeta^{i+1}_{m,n}, & x_{m-\frac{1}{2}} < x \leq x_{m+\frac{1}{2}}\ , y_{n-\frac{1}{2}} < y \leq y_{n+\frac{1}{2}},\\ & 1 \leq m \leq N_x-1\ , 1 \leq n \leq N_y-1,\\ 0, & 0 \leq x \leq \frac{h_x}{2}\ ,\ L-\frac{h_x}{2} < x \leq L,\\ & 0 \leq y \leq \frac{h_y}{2}\ ,\ L-\frac{h_y}{2} < y \leq L. \end{cases} \tag{6.49}$$

The expression of $\zeta^{i+1}(x,y)$ as a Fourier series is as follows

$$\zeta^{i+1}(x,y) = \sum_{k_1=-\infty}^{\infty}\sum_{k_2=-\infty}^{\infty}\vartheta^{i+1}(k_1,k_2)e^{2\pi\iota\left(\frac{k_1x+k_2y}{L}\right)},\ 0 \leq i \leq N_t-1, \tag{6.50}$$

where

$$\vartheta^{i+1}(k_1,k_2)=\frac{1}{L^2}\int_0^L\int_0^L\zeta^{i+1}(x,y)e^{-2\pi\iota\left(\frac{k_1x+k_2y}{L}\right)}dxdy. \tag{6.51}$$

By virtue of the $\mathcal{L}_2$-discrete norm definition and Parseval's equality, we have

$$\|\zeta^{i+1}\|_2^2=\sum_{m=1}^{N_x-1}\sum_{n=1}^{N_y-1}h_xh_y|\zeta_{m,n}^{i+1}|^2=L^2\sum_{k_1=-\infty}^{\infty}\sum_{k_2=-\infty}^{\infty}|\vartheta^{i+1}(k_1,k_2)|^2. \tag{6.52}$$

Let us consider the form of the solution of equation (6.48) to be

$$\zeta_{m,n}^{i+1}=\vartheta^{i+1}e^{\iota(\varsigma_1mh_x+\varsigma_2nh_y)}, \tag{6.53}$$

where $\iota=\sqrt{-1},\ \varsigma_1=\frac{2\pi k_1}{L},\ \varsigma_2=\frac{2\pi k_2}{L}$.

It is readily apparent that

$$\begin{cases}\mathcal{H}_x\zeta_{m,n}^{i+1}=\frac{1}{3}\left[\cos^2\left(\frac{\varsigma_1h_x}{2}\right)+2\right]\vartheta^{i+1}e^{\iota(\varsigma_1mh_x+\varsigma_2nh_y)},\\ \mathcal{H}_y\zeta_{m,n}^{i+1}=\frac{1}{3}\left[\cos^2\left(\frac{\varsigma_2h_y}{2}\right)+2\right]\vartheta^{i+1}e^{\iota(\varsigma_1mh_x+\varsigma_2nh_y)},\\ \delta_x^2\zeta_{m,n}^{i+1}=-\frac{4}{h_x^2}\sin^2\left(\frac{\varsigma_1h_x}{2}\right)\vartheta^{i+1}e^{\iota(\varsigma_1mh_x+\varsigma_2nh_y)},\\ \delta_y^2\zeta_{m,n}^{i+1}=-\frac{4}{h_y^2}\sin^2\left(\frac{\varsigma_2h_y}{2}\right)\vartheta^{i+1}e^{\iota(\varsigma_1mh_x+\varsigma_2nh_y)}.\end{cases} \tag{6.54}$$

By inserting equation (6.53) into equation (6.48) and using equations given in (6.54), we ascertain that

$$\left(a_1+\frac{\sigma\lambda_1}{\nu}b_1\right)\left(a_2+\frac{\sigma\lambda_2}{\nu}b_2\right)\vartheta^{i+1}=\frac{a_1a_2}{\nu}\left[\sum_{k=1}^{i}\left(w_{i,k}^{(\alpha,\sigma)}-w_{i,k-1}^{(\alpha,\sigma)}\right)\vartheta^k+w_{i,0}^{(\alpha,\sigma)}\vartheta^0\right]$$
$$-\frac{(1-\sigma)}{\nu}\left(\lambda_1a_2b_1+\lambda_2a_1b_2+\mu_ra_1a_2\right)\vartheta^i+\frac{\sigma^2}{\nu^2}\lambda_1\lambda_2b_1b_2\vartheta^i,\ 0\le i\le N_t-1, \tag{6.55}$$

where

$$\begin{cases} a_1 = \frac{1}{3}\left[\cos^2\left(\frac{\varsigma_1 h_x}{2}\right) + 2\right],\ b_1 = \frac{4}{h_x^2}\sin^2\left(\frac{\varsigma_1 h_x}{2}\right), \\ a_2 = \frac{1}{3}\left[\cos^2\left(\frac{\varsigma_2 h_y}{2}\right) + 2\right],\ b_2 = \frac{4}{h_y^2}\sin^2\left(\frac{\varsigma_2 h_y}{2}\right). \end{cases} \tag{6.56}$$

Here, it is easy to understand that $a_1, a_2 \geq \frac{2}{3}$, and $b_1, b_2 \geq 0$.

Rewriting equation (6.55), we have

$$\begin{aligned} \vartheta^{i+1} =& \frac{1}{\left(a_1 + \frac{\sigma\lambda_1}{\nu}b_1\right)\left(a_2 + \frac{\sigma\lambda_2}{\nu}b_2\right)}\left[\frac{a_1a_2}{\nu}\left(\sum_{k=1}^{i}\left(w_{i,k}^{(\alpha,\sigma)} - w_{i,k-1}^{(\alpha,\sigma)}\right)\vartheta^k + w_{i,0}^{(\alpha,\sigma)}\vartheta^0\right)\right. \\ & \left. - \frac{(1-\sigma)}{\nu}\left(\lambda_1a_2b_1 + \lambda_2a_1b_2 + \mu_r a_1a_2\right)\vartheta^i + \frac{\sigma^2}{\nu^2}\lambda_1\lambda_2b_1b_2\vartheta^i\right],\ 0 \leq i \leq N_t - 1. \end{aligned} \tag{6.57}$$

Lemma 6.6. *Consider ϑ^{i+1} to be the solution of equation (6.57). Then,*

$$|\vartheta^{i+1}| \leq |\vartheta^0|,\ 0 \leq i \leq N_t - 1.$$

Proof. We shall establish the validity of this statement by employing the principle of mathematical induction. By substituting $i = 0$ into equation (6.57), we obtain

$$\vartheta^1 = \frac{\left[\frac{a_1a_2}{\nu}w_{0,0}^{(\alpha,\sigma)} - \frac{(1-\sigma)}{\nu}\left(\lambda_1a_2b_1 + \lambda_2a_1b_2 + \mu_r a_1a_2\right) + \frac{\sigma^2}{\nu^2}\lambda_1\lambda_2b_1b_2\right]\vartheta^0}{\left(a_1 + \frac{\sigma\lambda_1}{\nu}b_1\right)\left(a_2 + \frac{\sigma\lambda_2}{\nu}b_2\right)}. \tag{6.58}$$

Since $\sigma \geq (1-\sigma) \geq 0$ and $w_{0,0}^{(\alpha,\sigma)} > 0$, therefore

$$|\vartheta^1| \leq \frac{\left[\frac{a_1a_2}{\nu}(\mu_r\sigma + w_{0,0}^{(\alpha,\sigma)}) + \frac{\sigma}{\nu}\left(\lambda_1a_2b_1 + \lambda_2a_1b_2\right) + \frac{\sigma^2}{\nu^2}\lambda_1\lambda_2b_1b_2\right]|\vartheta^0|}{\left(a_1 + \frac{\sigma\lambda_1}{\nu}b_1\right)\left(a_2 + \frac{\sigma\lambda_2}{\nu}b_2\right)} \leq |\vartheta^0|. \tag{6.59}$$

Now, let us assume that

$$|\vartheta^l| \leq |\vartheta^0|, \text{ for all } 1 \leq l \leq i. \tag{6.60}$$

Next, for $l = i+1$, from equation (6.57) with Lemma 6.1 and assumptions (6.60), we get

$$|\vartheta^{i+1}| \leq \frac{\left[\frac{a_1a_2}{\nu}\left(\sum_{k=1}^{i}\left(w_{i,k}^{(\alpha,\sigma)} - w_{i,k-1}^{(\alpha,\sigma)}\right) + w_{i,0}^{(\alpha,\sigma)}\right) + \frac{(1-\sigma)}{\nu}\left(\lambda_1a_2b_1 + \lambda_2a_1b_2 + \mu_ra_1a_2\right)\right]}{\left(a_1 + \frac{\sigma\lambda_1}{\nu}b_1\right)\left(a_2 + \frac{\sigma\lambda_2}{\nu}b_2\right)}|\vartheta^0|$$
$$+ \frac{\frac{\sigma^2}{\nu^2}\lambda_1\lambda_2b_1b_2}{\left(a_1 + \frac{\sigma\lambda_1}{\nu}b_1\right)\left(a_2 + \frac{\sigma\lambda_2}{\nu}b_2\right)}|\vartheta^0|$$

Since $\sigma \geq (1-\sigma) \geq 0$ and $w_{i,i}^{(\alpha,\sigma)} > 0$, therefore

$$|\vartheta^{i+1}| \leq \frac{\left[\frac{a_1a_2}{\nu}\left(\mu_r\sigma + w_{i,i}^{(\alpha,\sigma)}\right) + \frac{\sigma}{\nu}\left(\lambda_1a_2b_1 + \lambda_2a_1b_2\right) + \frac{\sigma^2}{\nu^2}\lambda_1\lambda_2b_1b_2\right]}{\left(a_1 + \frac{\sigma\lambda_1}{\nu}b_1\right)\left(a_2 + \frac{\sigma\lambda_2}{\nu}b_2\right)}|\vartheta^0| = |\vartheta^0|.$$

Thus, we have $|\vartheta^{i+1}| \leq |\vartheta^0|$, for all $0 \leq i \leq N_t - 1$. □

Theorem 6.2. *The high-order compact ADI scheme given by (6.29) for solving the model problem (6.7)-(6.8) is unconditionally stable.*

Proof. By considering equation (6.52) and Lemma 6.6 together, one can obtain the following inequality

$$\|\zeta^{i+1}\|_2^2 = L^2\sum_{k_1=-\infty}^{\infty}\sum_{k_2=-\infty}^{\infty}|\vartheta^{i+1}(k_1,k_2)|^2 \leq L^2\sum_{k_1=-\infty}^{\infty}\sum_{k_2=-\infty}^{\infty}|\vartheta^0(k_1,k_2)|^2 = \|\zeta^0\|_2^2.$$

Thus, $\|\zeta^{i+1}\|_2 \leq \|\zeta^0\|_2,\ 0 \leq i \leq N_t - 1$. Hence, the numerical scheme given by (6.29) is unconditionally stable. □

6.2.3 Convergence analysis

In this part, we aim to assess the convergence of the proposed scheme (6.29) with respect to the model problem (6.7)-(6.8).

By subtracting (6.29) from (6.27), we obtain

$$\left(\mathcal{H}_x - \frac{\sigma\lambda_1}{\nu}\delta_x^2\right)\left(\mathcal{H}_y - \frac{\sigma\lambda_2}{\nu}\delta_y^2\right)\epsilon_{m,n}^{i+1} = \frac{1}{\nu}\left[\sum_{k=1}^{i}\left(w_{i,k}^{(\alpha,\sigma)} - w_{i,k-1}^{(\alpha,\sigma)}\right)\mathcal{H}_x\mathcal{H}_y\epsilon_{m,n}^{k}\right]$$
$$- \frac{\mu_r(1-\sigma)}{\nu}\mathcal{H}_x\mathcal{H}_y\epsilon_{m,n}^{i} + \frac{(1-\sigma)}{\nu}\left(\lambda_1\mathcal{H}_y\delta_x^2 + \lambda_2\mathcal{H}_x\delta_y^2\right)\epsilon_{m,n}^{i} + \frac{\lambda_1\lambda_2\sigma^2}{\nu^2}\delta_x^2\delta_y^2\epsilon_{m,n}^{i}$$
$$+ (\mathcal{R}_f)_{m,n}^{i+1},\ 1 \leq m \leq N_x - 1,\ 1 \leq n \leq N_y - 1,\ 0 \leq\ i \leq N_t - 1, \tag{6.61}$$

where

$$\begin{cases} \epsilon_{m,n}^{i} = v_{m,n}^{i} - V_{m,n}^{i},\ \ 1 \leq m \leq N_x - 1,\ 1 \leq n \leq N_y - 1,\ 1 \leq\ i \leq N_t, \\ \epsilon_{m,n}^{0} = 0,\ 0 \leq m \leq N_x,\ 0 \leq n \leq N_y, \\ \epsilon_{0,n}^{i} = \epsilon_{N_x,n}^{i},\ 0 \leq n \leq N_y,\ 1 \leq\ i \leq N_t, \\ \epsilon_{m,0}^{i} = \epsilon_{m,N_y}^{i},\ 0 \leq m \leq N_x,\ 1 \leq\ i \leq N_t. \end{cases} \tag{6.62}$$

Now, we define the grid functions $\epsilon^{i+1}(x,y)$ and $\mathcal{R}_f^{i+1}(x,y)$ for $0 \leq i \leq N_t - 1$ as follows

$$\epsilon^{i+1}(x,y) = \begin{cases} \epsilon_{m,n}^{i+1}, & x_{m-\frac{1}{2}} < x \leq x_{m+\frac{1}{2}}, y_{n-\frac{1}{2}} < y \leq y_{n+\frac{1}{2}}, \\ & 1 \leq m \leq N_x - 1, 1 \leq n \leq N_y - 1, \\ 0, & 0 \leq x \leq \frac{h_x}{2}, L - \frac{h_x}{2} < x \leq L, \\ & 0 \leq y \leq \frac{h_y}{2}, L - \frac{h_y}{2} < y \leq L, \end{cases}$$

and

$$\mathcal{R}_f^{i+1}(x,y) = \begin{cases} (\mathcal{R}_f)_{m,n}^{i+1}, & x_{m-\frac{1}{2}} < x \leq x_{m+\frac{1}{2}}, y_{n-\frac{1}{2}} < y \leq y_{n+\frac{1}{2}}, \\ & 1 \leq m \leq N_x - 1, 1 \leq n \leq N_y - 1, \\ 0, & 0 \leq x \leq \frac{h_x}{2}, L - \frac{h_x}{2} < x \leq L, \\ & 0 \leq y \leq \frac{h_y}{2}, L - \frac{h_y}{2} < y \leq L. \end{cases}$$

The expressions of $\epsilon^{i+1}(x,y)$ and $\mathcal{R}_f^{i+1}(x,y)$ as a Fourier series are as follows

$$\epsilon^{i+1}(x,y) = \sum_{k_1=-\infty}^{\infty}\sum_{k_2=-\infty}^{\infty} \xi^{i+1}(k_1,k_2)e^{2\pi\iota\left(\frac{k_1x+k_2y}{L}\right)},$$
$$\mathcal{R}_f^{i+1}(x,y) = \sum_{k_1=-\infty}^{\infty}\sum_{k_2=-\infty}^{\infty} \chi^{i+1}(k_1,k_2)e^{2\pi\iota\left(\frac{k_1x+k_2y}{L}\right)},$$

where

$$\xi^{i+1}(k_1,k_2) = \frac{1}{L^2}\int_0^L\int_0^L \epsilon^{i+1}(x,y)e^{-2\pi\iota\left(\frac{k_1x+k_2y}{L}\right)}dxdy,$$
$$\chi^{i+1}(k_1,k_2) = \frac{1}{L^2}\int_0^L\int_0^L \mathcal{R}_f^{i+1}(x,y)e^{-2\pi\iota\left(\frac{k_1x+k_2y}{L}\right)}dxdy.$$

By virtue of the $\mathcal{L}_2$-discrete norm definition and Parseval's equality, we have

$$\|\epsilon^{i+1}\|_2^2 = \sum_{m=1}^{N_x-1}\sum_{n=1}^{N_y-1} h_xh_y|\epsilon_{m,n}^{i+1}|^2 = L^2\sum_{k_1=-\infty}^{\infty}\sum_{k_2=-\infty}^{\infty}|\xi^{i+1}(k_1,k_2)|^2, \tag{6.63}$$
$$\|\mathcal{R}_f^{i+1}\|_2^2 = \sum_{m=1}^{N_x-1}\sum_{n=1}^{N_y-1} h_xh_y|(\mathcal{R}_f)_{m,n}^{i+1}|^2 = L^2\sum_{k_1=-\infty}^{\infty}\sum_{k_2=-\infty}^{\infty}|\chi^{i+1}(k_1,k_2)|^2, \tag{6.64}$$

for $0 \leq i \leq N_t - 1$, where

$$\epsilon^{i+1} = \Big[\epsilon_{1,1}^{i+1}, \epsilon_{1,2}^{i+1}, \ldots, \epsilon_{1,N_y-1}^{i+1}, \epsilon_{2,1}^{i+1}, \epsilon_{2,2}^{i+1}, \ldots, \epsilon_{2,N_y-1}^{i+1}, \ldots, \epsilon_{N_x-1,1}^{i+1}, \epsilon_{N_x-1,2}^{i+1}, \ldots, \epsilon_{N_x-1,N_y-1}^{i+1}\Big],$$

$$\mathcal{R}_f^{i+1} = \Big[(\mathcal{R}_f)_{1,1}^{i+1}, (\mathcal{R}_f)_{1,2}^{i+1}, \ldots, (\mathcal{R}_f)_{1,N_y-1}^{i+1}, (\mathcal{R}_f)_{2,1}^{i+1}, (\mathcal{R}_f)_{2,2}^{i+1}, \ldots, (\mathcal{R}_f)_{2,N_y-1}^{i+1}, \ldots,$$
$$(\mathcal{R}_f)_{N_x-1,1}^{i+1}, (\mathcal{R}_f)_{N_x-1,2}^{i+1}, \ldots, (\mathcal{R}_f)_{N_x-1,N_y-1}^{i+1}\Big]^T.$$

Let the solutions $\epsilon_{m,n}^{i+1}$ and $(\mathcal{R}_f)_{m,n}^{i+1}$ have following form

$$\epsilon_{m,n}^{i+1} = \xi^{i+1} e^{\iota(\varsigma_1 m h_x + \varsigma_2 n h_y)}, \quad (\mathcal{R}_f)_{m,n}^{i+1} = \chi^{i+1} e^{\iota(\varsigma_1 m h_x + \varsigma_2 n h_y)}, \tag{6.65}$$

where $\iota = \sqrt{-1}$, $\varsigma_1 = \frac{2\pi k_1}{L}$, $\varsigma_2 = \frac{2\pi k_2}{L}$. It is readily apparent that

$$\begin{cases} \mathcal{H}_x \epsilon_{m,n}^i = \frac{1}{3}\left[\cos^2\left(\frac{\varsigma_1 h_x}{2}\right) + 2\right] \xi^i e^{\iota(\varsigma_1 m h_x + \varsigma_2 n h_y)}, \\ \mathcal{H}_y \epsilon_{m,n}^i = \frac{1}{3}\left[\cos^2\left(\frac{\varsigma_2 h_y}{2}\right) + 2\right] \xi^i e^{\iota(\varsigma_1 m h_x + \varsigma_2 n h_y)}, \\ \delta_x^2 \epsilon_{m,n}^i = -\frac{4}{h_x^2}\sin^2\left(\frac{\varsigma_1 h_x}{2}\right) \xi^i e^{\iota(\varsigma_1 m h_x + \varsigma_2 n h_y)}, \\ \delta_y^2 \epsilon_{m,n}^i = -\frac{4}{h_y^2}\sin^2\left(\frac{\varsigma_2 h_y}{2}\right) \xi^i e^{\iota(\varsigma_1 m h_x + \varsigma_2 n h_y)}. \end{cases} \tag{6.66}$$

By inserting equation (6.65) into equation (6.61), using $\xi^0 = 0$, and equations given in (6.66), we ascertain that

$$\xi^{i+1} = \frac{\frac{a_1 a_2}{\nu}\left(\sum_{k=1}^{i}(w_{i,k}^{(\alpha,\sigma)} - w_{i,k-1}^{(\alpha,\sigma)})\xi^k\right) - \frac{(1-\sigma)}{\nu}(\lambda_1 a_2 b_1 + \lambda_2 a_1 b_2 + \mu_r a_1 a_2)\xi^i}{\left(a_1 + \frac{\sigma\lambda_1}{\nu} b_1\right)\left(a_2 + \frac{\sigma\lambda_2}{\nu} b_2\right)}$$
$$+ \frac{\frac{\sigma^2}{\nu^2}\lambda_1\lambda_2 b_1 b_2 \xi^i + \chi^{i+1}}{\left(a_1 + \frac{\sigma\lambda_1}{\nu} b_1\right)\left(a_2 + \frac{\sigma\lambda_2}{\nu} b_2\right)}. \tag{6.67}$$

As a result of the convergence exhibited by the series on the right hand side of equation (6.64), it follows that there exists a positive value $c > 0$ satisfying

$$|\chi^{i+1}| \equiv |\chi^{i+1}(k_1, k_2)| \leq c\Delta t |\chi^1(k_1, k_2)| \equiv c\Delta t |\chi^1|, \ 0 \leq i \leq N_t - 1, \tag{6.68}$$

where $\Delta t = \max\limits_{1 \leq i \leq N_t} \Delta t_i$.

Lemma 6.7. *For $i = 0, 1, \ldots, N_t - 1$, we have*

$$|\xi^{i+1}| \leq \frac{9}{4}c(1+\Delta t)^{i+1}|\chi^1|, \ 0 \leq i \leq N_t - 1, \tag{6.69}$$

where c is a constant in (6.68).

Proof. We shall establish the validity of this statement by employing the principle of mathematical induction. By substituting $i = 0$ and using $\xi^0 = 0$ into equation (6.67), we obtain

$$\xi^1 = \frac{\chi^1}{\left(a_1 + \frac{\sigma\lambda_1}{\nu}b_1\right)\left(a_2 + \frac{\sigma\lambda_2}{\nu}b_2\right)}.$$

By utilizing equation (6.69) along with the provided conditions $a_1, a_2 \geq \frac{2}{3}$ and $b_1, b_2 \geq 0$, we can conclude

$$|\xi^1| \leq \frac{9}{4}c(1+\Delta t)|\chi^1|. \tag{6.70}$$

Now, let us assume that

$$|\xi^l| \leq \frac{9}{4}c(1+\Delta t)^l|\chi^1|, \ \text{for all } 1 \leq l \leq i. \tag{6.71}$$

Next, for $l = i+1$, from equation (6.67) with Lemma 6.1, and equation (6.68), we get

$$\begin{aligned}|\xi^{i+1}| =& \frac{1}{\left(a_1 + \frac{\sigma\lambda_1}{\nu}b_1\right)\left(a_2 + \frac{\sigma\lambda_2}{\nu}b_2\right)}\left[\frac{a_1a_2}{\nu}\left(\sum_{k=1}^{i}\left(w_{i,k}^{(\alpha,\sigma)} - w_{i,k-1}^{(\alpha,\sigma)}\right)\right)\max_{1\leq j\leq i}|\xi^j| + \frac{(1-\sigma)}{\nu}\right.\\ &\left.\times\left(\lambda_1a_2b_1 + \lambda_2a_1b_2 + \mu_ra_1a_2\right)|\xi^i| + \frac{\sigma^2}{\nu^2}\lambda_1\lambda_2b_1b_2|\xi^i| + c\Delta t|\chi^1|\right].\end{aligned}$$

Further, using the assumptions (6.71) and $\sigma \geq (1-\sigma) \geq 0$, we get

$$|\xi^{i+1}| \leq \frac{1}{\left(a_1 + \frac{\sigma\lambda_1}{\nu} b_1\right)\left(a_2 + \frac{\sigma\lambda_2}{\nu} b_2\right)} \Bigg[\Bigg(\frac{a_1 a_2}{\nu}\left(w_{i,i}^{(\alpha,\sigma)} - w_{i,0}^{(\alpha,\sigma)}\right) + \frac{\sigma}{\nu}(\lambda_1 a_2 b_1 + \lambda_2 a_1 b_2 \\ + \mu_r a_1 a_2) + \frac{\sigma^2}{\nu^2}\lambda_1\lambda_2 b_1 b_2\Bigg)\left(\frac{9}{4}c(1+\Delta t)^i |\chi^1|\right) + c\Delta t|\chi^1|\Bigg].$$

Again, by invoking Lemma 6.1, we have

$$|\xi^{i+1}| \leq \frac{9}{4}c\Big\{(1+\Delta t)^i + \Delta t\Big\}|\chi^1| \leq \frac{9}{4}c(1+\Delta t)^{i+1}|\chi^1|.$$

Thus, we have the Lemma. □

Theorem 6.3. *Assume that the problem (6.7)-(6.8) has a solution $v(x,y,t)$, which meets the assumptions provided in (6.3)-(6.5) and let $V = \{V_{m,n}^i \mid 0 \leq m \leq N_x, 0 \leq n \leq N_y, 1 \leq i \leq N_t\}$ be the solution of the high-order compact ADI scheme given by (6.29). Then, we have*

$$\|v^{i+1} - V^{i+1}\|_2 \leq \hat{c}\left(N_t^{-\min\{3-\alpha,\theta\alpha,1+2\alpha,2+\alpha\}} + h_x^4 + h_y^4\right),\ 0 \leq i \leq N_t - 1,$$

where $\hat{c} = \frac{9}{4}c^2 L\exp(2T_f)$.

Proof. Utilizing both Theorem 6.1 and the first equality of (6.64), we arrive at

$$\begin{aligned}\|\mathcal{R}_f^{i+1}\|_2 &\leq c\sqrt{N_x h_x}\sqrt{N_y h_y}\left(N_t^{-\min\{3-\alpha,\theta\alpha,1+2\alpha,2+\alpha\}} + h_x^4 + h_y^4\right) \\ &\leq cL\left(N_t^{-\min\{3-\alpha,\theta\alpha,1+2\alpha,2+\alpha\}} + h_x^4 + h_y^4\right),\ 0 \leq i \leq N_t - 1. \qquad (6.72)\end{aligned}$$

By invoking Lemma 6.7, along with equations (6.63), (6.64), and (6.72), for $0 \leq i \leq N_t - 1$, we can deduce the following estimate

$$
\begin{aligned}
\|\epsilon^{i+1}\|_2^2 &= L^2 \sum_{k_1=-\infty}^{\infty} \sum_{k_2=-\infty}^{\infty} |\xi^{i+1}(k_1,k_2)|^2 \\
&\leq L^2 \sum_{k_1=-\infty}^{\infty} \sum_{k_2=-\infty}^{\infty} \left(\frac{9}{4}c\right)^2 (1+\Delta t)^{2(i+1)} |\chi^1(k_1,k_2)|^2 \\
&= \left(\frac{9}{4}c\right)^2 (1+\Delta t)^{2(i+1)} \|\mathcal{R}_f^1\|_2^2 \\
&\leq (cL)^2 \left(\frac{9}{4}c\right)^2 (1+\Delta t)^{2(i+1)} \left(N_t^{-\min\{3-\alpha,\theta\alpha,1+2\alpha,2+\alpha\}} + h_x^4 + h_y^4\right)^2.
\end{aligned}
$$

Moreover, by noting the fact that $\Delta t, i\Delta t \leq T_f$, we obtain

$$
\|\epsilon^{i+1}\|_2 \leq \hat{c} \left(N_t^{-\min\{3-\alpha,\theta\alpha,1+2\alpha,2+\alpha\}} + h_x^4 + h_y^4\right),
$$

where $\hat{c} = \frac{9}{4}c^2 L \exp(2T_f)$.

Henceforth, the theorem holds. $\square$

6.3 Numerical results

This section is dedicated to presenting the results obtained from a comprehensive numerical illustration, chosen to appraise the practical implementation of the proposed numerical method. If $u(x_m, y_n, t_i)$ and $U(x_m, y_n, t_i)$ are the exact and approximate solutions of problem (6.1)-(6.2), respectively, at (x_m, y_n, t_i), then the accuracy of the numerical solution will be carried out according to the following norms

$$
\mathcal{L}_\infty = \|\mathcal{L}(h_x, h_y, \Delta t)\|_\infty = \max_{1\leq i\leq N_t} \left[\max_{\substack{1\leq m\leq N_x-1 \\ 1\leq n\leq N_y-1}} \left|U_{m,n}^i - u(x_m, y_n, t_i)\right| \right], \tag{6.73}
$$

$$\mathcal{L}_2 = \|\mathcal{L}(h_x, h_y, \Delta t)\|_2 = \max_{1\leq i\leq N_t} \left[\sum_{m=1}^{N_x-1} \sum_{n=1}^{N_y-1} h_x h_y \left| U^i_{m,n} - u(x_m, y_n, t_i) \right|^2 \right]^{\frac{1}{2}}. \tag{6.74}$$

We employ the following formula to measure the order of convergence

$$\text{cov.order} = \begin{cases} log_2\left(\frac{\mathcal{L}_l(2h_x, 2h_y, \Delta t)}{\mathcal{L}_l(h_x, h_y, \Delta t)}\right), & \text{in space}, \\ log_2\left(\frac{\mathcal{L}_l(h_x, h_y, 2\Delta t)}{\mathcal{L}_l(h_x, h_y, \Delta t)}\right), & \text{in time}, \end{cases} \tag{6.75}$$

where $l = \infty$ or 2.

To perform the numerical computations, we take $T = \max\{2^{-\theta}T_f, (1 - 1/\theta)T_f\}$, $\Upsilon = \max\left\{\frac{\theta}{2^\theta - 1 + \theta}, \frac{\theta(\theta-1)}{1+\theta(\theta-1)}\right\}$, $\hat{N}_t = \lceil \Upsilon N_t \rceil$, and subdivide the interval $[T, T_f]$ into a uniform grid with a time-width $\Delta t = \frac{T_f - T}{N_t - \hat{N}_t} \geq \Delta t_{\hat{N}_t}$. In this way, the complete mesh $\{t_i\}_{i=0}^{N_t}$ fulfills the mesh conditions stated in Lemmas 6.1 and 6.4. Moreover, to avoid inaccuracies due to roundoff, we utilize adaptive Gauss-Kronrod quadrature (based on the methodology from [69]) for the computation of coefficients $r_{i,k}^{(\alpha,\sigma)}$ and $s_{i,k}^{(\alpha,\sigma)}$ in equations (6.12) and (6.13).

Example 6.1. *[93] Numerical calculations are carried out to examine the accuracy of the assumption that the function* $u(x, y, t) = t^\alpha \exp(x + y)$ *represents the exact solution for problem (6.1)–(6.2) with* $L = 1$, $T_f = 1$, *and the coefficients* $\lambda_1 = \lambda_2 = 1$, $\mu_1 = \mu_2 = -1$, $\gamma = 0$. *Also, the source function for this test problem is specified as follows*

$$f(x, y, t) = \frac{\pi\alpha \csc(\pi\alpha)}{\Gamma(1-\alpha)} \exp(x + y).$$

It is important to note that, at $t = 0$ *the exact solution, in this case, exhibits non-smooth behavior.*

TABLE 6.1: (Example 6.1) $\mathcal{L}_\infty$ and $\mathcal{L}_2$ errors with temporal order of convergence for $\alpha = 0.2$, $N_x = N_y = 10$.

θ	N_t	$\mathcal{L}_\infty$-error	cov.order$_t$	$\mathcal{L}_2$-error	cov.order$_t$	CPU time (s)	Optimal order
1	80	3.9088e-03		2.1297e-03		3.9089	0.2
	160	4.0434e-03		2.2081e-03		10.946	
	320	4.1823e-03		2.2900e-03		87.117	
	640	4.3186e-03		2.3717e-03		300.05	
$\frac{3-\alpha}{\alpha}$	80	1.0196e-04	-	5.7456e-05	-	4.7981	1.4
	160	4.6961e-05	1.1184	2.6546e-05	1.1139	21.524	
	320	2.8254e-05	0.7330	1.5824e-05	0.7463	75.203	
	640	1.0676e-05	1.4040	6.0363e-06	1.3904	295.50	
$\frac{1+2\alpha}{\alpha}$	80	3.4511e-04	-	2.3273e-04	-	3.6269	1.4
	160	1.4842e-04	1.2173	9.8927e-05	1.2342	11.958	
	320	6.4051e-05	1.2124	3.9820e-05	1.3128	73.749	
	640	2.7240e-05	1.2334	1.5496e-05	1.3615	285.81	
$\frac{2+\alpha}{\alpha}$	80	7.8517e-05	-	4.4318e-05	-	4.8860	1.4
	160	4.1935e-05	0.9048	2.3571e-05	0.9108	20.667	
	320	2.0824e-05	1.0099	1.1704e-05	1.0099	77.560	
	640	8.0054e-06	1.3792	4.5287e-06	1.3699	307.41	

The implementation of the proposed scheme (6.29) has been carried out on this test example, considering different values of the fractional order α, as well as varying discretization parameters N_x, N_y, and N_t. The temporal order of convergence is presented in Tables 6.1, 6.2, 6.3, and 6.4 with respect to both the $\mathcal{L}_\infty$ and $\mathcal{L}_2$ norms. These tables provide the convergence orders for different α values of $0.2, 0.4, 0.6,$ and 0.8, considering various grading parameters $\theta = 1, \frac{3-\alpha}{\alpha}, \frac{1+2\alpha}{\alpha}$, and $\frac{2+\alpha}{\alpha}$. Upon analyzing the presented tables, a noteworthy observation arises. Specifically, when considering the temporal order of convergence for $\theta = 1$ (representing uniform spacing), it becomes apparent that the attained order of convergence falls below α. This discrepancy stems from the inherent nature of the problem's solution, which exhibits weak singularity at $t = 0$. Furthermore, through the utilization of a fitted mesh with various grading parameters, it has been observed that $\theta = \frac{(1+2\alpha)}{\alpha}$ demonstrates optimal grading behavior. This particular choice not only yields an optimal order of

TABLE 6.2: (Example 6.1) $\mathcal{L}_\infty$ and $\mathcal{L}_2$ errors with temporal order of convergence for $\alpha = 0.4$, $N_x = N_y = 10$.

θ	N_t	$\mathcal{L}_\infty$-error	cov.order$_t$	$\mathcal{L}_2$-error	cov.order$_t$	CPU Time (s)	Optimal order
1	80	7.0301e-03		3.9279e-03		3.7943	0.4
	160	7.0417e-03		3.9823e-03		14.391	
	320	6.8103e-03	0.04821	3.9105e-03	0.02621	40.947	
	640	6.3652e-03	0.09750	3.7144e-03	0.07424	174.07	
$\frac{3-\alpha}{\alpha}$	80	4.7165e-05	-	2.6684e-05	-	3.4720	1.8
	160	1.8508e-05	1.3495	1.0481e-05	1.3481	11.208	
	320	7.1996e-06	1.3622	4.0807e-06	1.3609	43.299	
	640	2.5924e-06	1.4736	1.4705e-06	1.4725	173.49	
$\frac{1+2\alpha}{\alpha}$	80	1.2512e-04	-	8.3041e-05	-	6.9270	1.8
	160	4.3879e-05	1.5116	2.5603e-05	1.6975	15.224	
	320	1.3608e-05	1.6890	7.6308e-06	1.7464	42.530	
	640	4.0908e-06	1.7339	2.2138e-06	1.7852	176.27	
$\frac{2+\alpha}{\alpha}$	80	5.0591e-05	-	2.8516e-05	-	3.6209	1.8
	160	1.5626e-05	1.6948	8.8507e-06	1.6879	11.596	
	320	6.0439e-06	1.3704	3.4272e-06	1.3687	41.970	
	640	2.3312e-06	1.3744	1.3223e-06	1.3739	178.07	

convergence, reaching $\min\{1+2\alpha, 3-\alpha\}$, but also outperforms alternative approximation [93] proposed in the literature on graded meshes, thereby establishing its superiority. Table 6.5 presents a comprehensive comparison between our proposed method and the approach outlined in reference [93]. Despite [93] being specifically designed to handle non-smooth solutions, our method outperforms it in terms of both error and temporal order of convergence. Moreover, the spatial orders of convergence with respect to $\mathcal{L}_\infty$ and $\mathcal{L}_2$ norms for fractional orders $\alpha = 0.2, 0.4, 0.6,$ and 0.8 are depicted in Table 6.6. Here, we have chosen the optimal grading parameter $\theta = \frac{(1+2\alpha)}{\alpha}$ and we vary time discretization parameter as $N_t = \lceil N_x^{4/(1+2\alpha)} \rceil$, taking different values of N_x and N_y. By examining this table, it becomes evident that the used compact finite difference scheme exhibits spatial accuracy of fourth order. Additionally, the CPU time in seconds has been provided in all the tables, showcasing the efficiency of our approach.

TABLE 6.3: (Example 6.1) $\mathcal{L}_\infty$ and $\mathcal{L}_2$ errors with temporal order of convergence for $\alpha = 0.6$, $N_x = N_y = 10$.

θ	N_t	$\mathcal{L}_\infty$-error	cov.order$_t$	$\mathcal{L}_2$-error	cov.order$_t$	CPU Time (s)	Optimal order
1	80	6.2719e-03	-	3.6877e-03	-	5.6311	0.6
	160	5.1852e-03	0.27451	3.1205e-03	0.24096	31.887	
	320	4.0000e-03	0.37438	2.4855e-03	0.32819	45.111	
	640	2.9158e-03	0.45612	1.8873e-03	0.39721	177.95	
$\frac{3-\alpha}{\alpha}$	80	3.0064e-05	-	1.9839e-05	-	4.1689	2.2
	160	6.9723e-06	2.1083	4.5875e-06	2.1126	10.443	
	320	1.6141e-06	2.1109	1.0019e-06	2.1948	38.252	
	640	5.0304e-07	1.6819	2.8538e-07	1.8118	172.28	
$\frac{1+2\alpha}{\alpha}$	80	4.1864e-05	-	2.7605e-05	-	4.9123	2.2
	160	1.0938e-05	1.9362	6.8509e-06	2.0105	11.694	
	320	2.7856e-06	1.9733	1.6214e-06	2.0790	42.528	
	640	6.6279e-07	2.0714	3.6787e-07	2.1399	152.71	
$\frac{2+\alpha}{\alpha}$	80	2.3718e-05	-	1.5418e-05	-	4.5374	2.2
	160	5.5975e-06	2.0831	3.4082e-06	2.1776	15.965	
	320	1.8262e-06	1.6158	1.0362e-06	1.7176	53.446	
	640	5.8081e-07	1.6527	3.2952e-07	1.6529	215.59	

Example 6.2. *[114] Numerical calculations are carried out to examine the accuracy of the assumption that the function* $u(x, y, t) = t^\alpha(\sin(x)\sin(y) + x(\pi - x)y(\pi - y))$ *represents the exact solution for problem (6.1)–(6.2) with* $L = \pi$, $T_f = 1$, *and the coefficients* $\lambda_1 = \lambda_2 = 1$, $\mu_1 = \mu_2 = 0$, $\gamma = 0$. *Also, the source function for this test problem is specified as follows*

$$f(x, y, t) = \Gamma(1+\alpha)(\sin x \sin y + x(\pi - x)y(\pi - y)) + t^\alpha \Big(2\sin x \sin y + 2\pi(x+y) - 2(x^2+y^2)\Big).$$

It is important to note that, at $t = 0$ *the exact solution, in this case, exhibits non-smooth behavior.*

The numerical outcomes for Example 6.2 are presented in Tables 6.7, 6.8, and 6.9.

TABLE 6.4: (Example 6.1) $\mathcal{L}_\infty$ and $\mathcal{L}_2$ errors with temporal order of convergence for $\alpha = 0.8$, $N_x = N_y = 10$.

θ	N_t	$\mathcal{L}_\infty$-error	cov.order$_t$	$\mathcal{L}_2$-error	cov.order$_t$	CPU Time (s)	Optimal order
1	80	2.4952e-03	-	1.5804e-03	-	4.7075	0.8
	160	1.6139e-03	0.62859	1.0595e-03	0.57689	11.881	
	320	1.0043e-03	0.68437	6.7614e-04	0.64800	43.437	
	640	6.2313e-04	0.68859	4.1767e-04	0.69496	171.27	
$\frac{3-\alpha}{\alpha}$	80	2.7483e-05	-	1.7910e-05	-	4.4918	2.2
	160	7.3489e-06	1.9029	4.7772e-06	1.9065	11.277	
	320	1.9127e-06	1.9419	1.2070e-06	1.9846	41.901	
	640	4.8590e-07	1.9769	2.9190e-07	2.0479	170.72	
$\frac{1+2\alpha}{\alpha}$	80	1.5602e-05	-	9.8260e-06	-	5.2718	2.2
	160	3.7209e-06	2.0680	2.3784e-06	2.0466	14.059	
	320	8.5331e-07	2.1245	5.4731e-07	2.1195	43.519	
	640	1.9151e-07	2.1556	1.2315e-07	2.1519	175.89	
$\frac{2+\alpha}{\alpha}$	80	1.3271e-05	-	8.1802e-06	-	4.6207	2.2
	160	3.0698e-06	2.1121	1.9071e-06	2.1007	12.104	
	320	6.9195e-07	2.1494	4.3211e-07	2.1419	44.024	
	640	1.5421e-07	2.1657	9.6601e-08	2.1612	178.02	

Table 6.7 provides a detailed view of the $\mathcal{L}_\infty$ and $\mathcal{L}_2$ errors along with the temporal order of convergence for different fractional orders α, all using the optimal mesh grading $\theta = \frac{(1+2\alpha)}{\alpha}$. The observations drawn from this table lead to the conclusion that the temporal order of convergence is precisely $\min\{1+2\alpha, 3-\alpha\}$. Additionally, in Table 6.8, we present a comparison of $\mathcal{L}_2$-errors between the proposed method and the one outlined in [114] for different fractional orders $\alpha = 0.2, 0.4, 0.6$, and 0.8. A careful examination of this table reveals that the errors obtained through our method are significantly lower compared to [114], showcasing superior performance. Moreover, Table 6.9 also provides an insightful comparison between our proposed method and the technique detailed in [114], offering the $\mathcal{L}_2$-error with spatial order of convergence for $\alpha = 0.8$ and $N_t = 4000$. The observations from this table undeniably reveal that our method yields significantly lower errors than [114]. Notably, our method achieves an impressive spatial order of convergence of four, far surpassing the

TABLE 6.5: (Example 6.1) Comparison with method in [93] taking $N_x = N_y = N_t$.

		Present method			Method in [93]		
α	N_t	$\mathcal{L}_\infty$-error	cov.order$_t$	CPU Time (s)	$\mathcal{L}_\infty$-error	cov.order$_t$	CPU Time (s)
0.3	2^5	7.9499e-04	-	0.6966	0.0019	-	0.674
	2^6	3.0782e-04	1.3270	2.3940	6.4899e-04	1.5497	5.017
	2^7	1.1381e-04	1.4402	16.921	2.1661e-04	1.5831	68.16
	2^8	4.0120e-05	1.5043	162.12	7.0716e-05	1.6150	1050.04
0.5	2^5	3.5441e-04	-	0.8617	0.0024	-	0.522
	2^6	1.0479e-04	1.7578	2.1709	9.0762e-04	1.4029	1.411
	2^7	2.9808e-05	1.8137	15.231	3.3360e-04	1.4440	13.15
	2^8	8.0640e-06	1.8861	144.22	1.2114e-04	1.4614	207.36
0.8	2^5	9.3635e-05	-	0.6867	0.0026	-	0.788
	2^6	2.4492e-05	1.9346	2.2374	0.0012	1.1122	5.003
	2^7	5.9577e-06	2.0395	16.203	5.3625e-04	1.1621	73.23
	2^8	1.3731e-06	2.1173	157.36	2.3608e-04	1.1836	1067.63

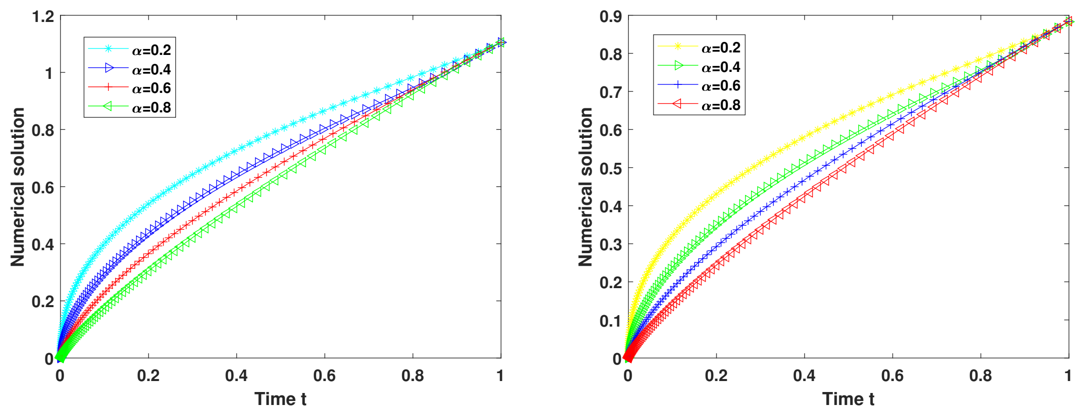

(i) Example 6.1 (ii) Example 6.2

FIGURE 6.1: Numerical solution for different values of α with $N_t = 100$ at $x = y = 0.1$.

spatial order of two reported in [114], thereby positioning itself as the superior choice. Figure 6.2 displays the maximum absolute errors obtained for various fractional order values $\alpha = 0.2, 0.4, 0.6$, and 0.8, comparing the results between a uniform mesh and a fitted mesh. Notably, the error on the fitted mesh is consistently lower than that on the uniform mesh. Moreover, as the fractional order increases from $\alpha = 0.2$ to 0.8, a

TABLE 6.6: (Example 6.1) $\mathcal{L}_\infty$ and $\mathcal{L}_2$ errors with spatial order of convergence for $N_t = \lceil N_x^{4/(1+2\alpha)} \rceil$.

α	$N_x = N_y$	$\mathcal{L}_\infty$-error	cov.order$_x$	$\mathcal{L}_2$-error	cov.order$_x$	CPU Time (s)
0.3	2^3	7.4205e-05	-	4.3397e-05	-	14.231
	2^4	5.4395e-06	3.7699	2.9589e-06	3.8744	736.84
	2^5	3.5852e-07	3.9233	1.8978e-07	3.9626	21277
0.5	2^3	1.0547e-04	-	6.8982e-05	-	2.4263
	2^4	8.7137e-06	3.5975	5.2583e-06	3.7135	29.819
	2^5	6.2331e-07	3.8053	3.4777e-07	3.9183	472.31
	2^6	5.1394e-08	3.6003	2.8867e-08	3.5906	39431
0.7	2^3	1.2528e-04	-	8.0656e-05	-	1.6036
	2^4	1.2081e-05	3.3743	7.9880e-06	3.3358	8.9149
	2^5	9.8456e-07	3.6172	6.4843e-07	3.6228	86.227
	2^6	7.1656e-08	3.7803	4.6761e-08	3.7935	1168.1
0.9	2^3	4.0937e-05	-	2.6114e-05	-	2.2913
	2^4	3.9168e-06	3.3856	2.5497e-06	3.3564	21.951
	2^5	3.2271e-07	3.6013	2.1032e-07	3.5996	256.41
	2^6	2.4277e-08	3.7325	1.5784e-08	3.7360	5197.1

TABLE 6.7: (Example 6.2) $\mathcal{L}_\infty$ and $\mathcal{L}_2$ errors with temporal order of convergence for $N_x = N_y = 5$.

α	N_t	$\mathcal{L}_\infty$-error	cov.order$_t$	$\mathcal{L}_2$-error	cov.order$_t$	CPU Time (s)	Optimal order
0.3	2^5	5.3303e-02	-	9.5083e-02	-	0.5185	1.6
	2^6	1.9617e-02	1.4421	3.5275e-02	1.4305	0.9659	
	2^7	6.3344e-03	1.6308	1.1519e-02	1.6146	3.6001	
	2^8	1.9989e-03	1.6639	3.7407e-03	1.6226	13.659	
0.5	2^5	2.7624e-02		5.2320e-02	-	0.5000	2
	2^6	8.6642e-03	1.6728	1.6625e-02	1.6539	0.8929	
	2^7	2.4210e-03	1.8394	4.6912e-03	1.8253	3.4745	
	2^8	5.7439e-04	2.0755	1.1683e-03	2.0055	13.920	
0.7	2^5	1.1722e-02	-	2.2629e-02	-	0.4999	2.3
	2^6	3.0925e-03	1.9224	5.9958e-03	1.9161	0.9152	
	2^7	6.1485e-04	2.3305	1.2073e-03	2.3120	3.5433	
	2^8	1.1915e-04	2.3674	2.3847e-04	2.3399	14.242	

TABLE 6.8: (Example 6.2) $\mathcal{L}_2$-error with $N_x = N_y = N_t$

N_t	α	Proposed method	Method in [114]	α	Proposed method	Method in [114]
2^5	0.2	9.998e-02	9.919e-01	0.4	1.134e-01	5.054e-01
2^6		6.115e-02	8.032e-01		2.667e-02	3.846e-01
2^7		2.710e-02	6.573e-01		8.627e-03	2.968e-01
2^8		9.600e-03	5.442e-01		3.080e-03	2.304e-01
2^9		3.846e-03	4.557e-01		1.172e-03	1.790e-01
2^5	0.6	4.378e-02	2.616e-01	0.8	1.014e-02	9.910e-02
2^6		1.095e-02	1.791e-01		2.580e-03	6.021e-02
2^7		3.240e-03	1.221e-01		7.467e-04	3.599e-02
2^8		1.021e-03	8.260e-02		2.159e-04	2.129e-02
2^9		3.305e-04	5.551e-02		6.239e-05	1.250e-02

noticeable decrease in errors is witnessed, signifying an improved smoothness in the solution. Further, in Figure 6.1, the numerical solutions for both the Examples 6.1 and 6.2 for multiple values of α with $x = y = 0.1$ are plotted against time. From this figure, it is clear that the order of the fractional derivative plays an important role in solving the problems under consideration. One can also note that the solutions exhibit an initial layer at $t = 0$, which agrees with the theory.

TABLE 6.9: (Example 6.2) Comparison with method in [114] with $\alpha = 0.8$, $N_t = 4000$.

	Proposed method		Method in [114]	
$N_x = N_y$	$\mathcal{L}_2$-error	cov.order$_x$	$\mathcal{L}_2$-error	cov.order$_x$
2^2	1.5868e-03	-	5.055e-02	-
2^3	9.5959e-05	4.0475	1.246e-02	2.0204
2^4	3.9530e-06	4.6013	3.009e-03	2.0499

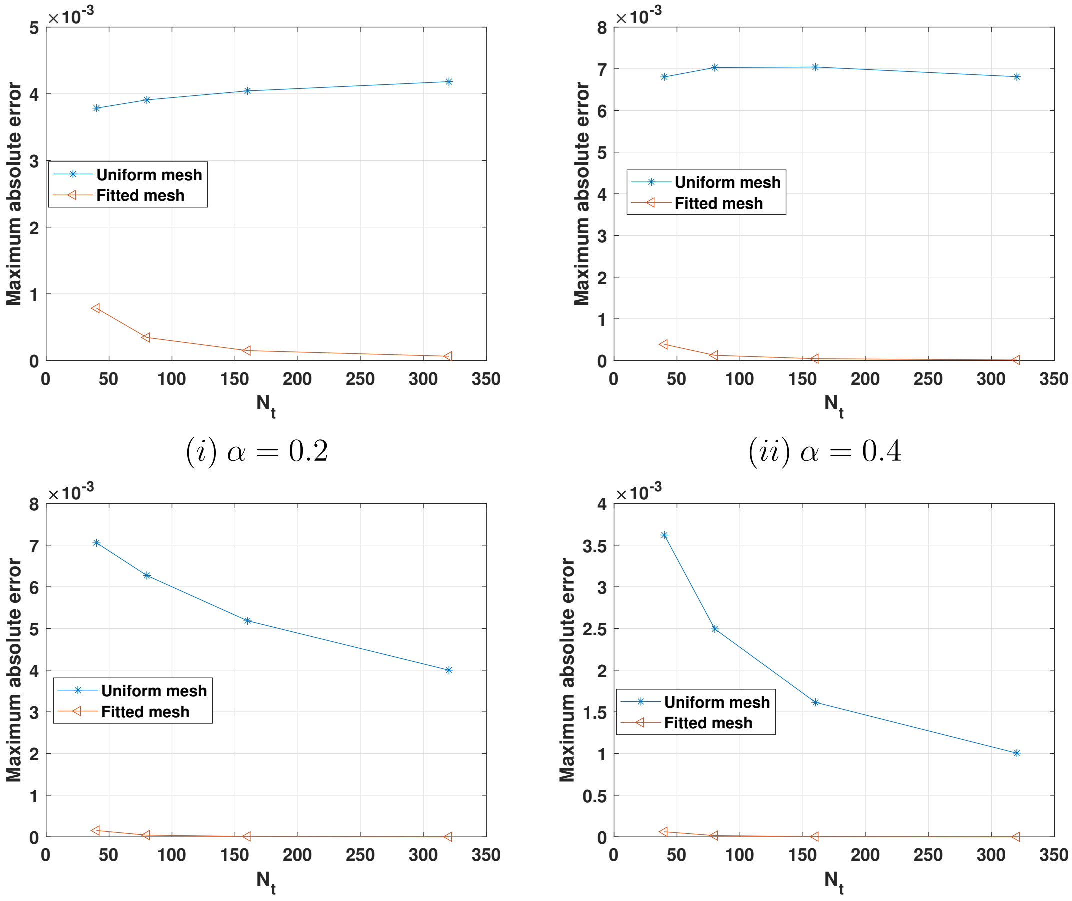

(*i*) $\alpha = 0.2$ (*ii*) $\alpha = 0.4$

(*iii*) $\alpha = 0.6$ (*iv*) $\alpha = 0.8$

FIGURE 6.2: Maximum absolute error using uniform and fitted meshes for different values of α with $N_x = N_y = 10$.

6.4 Conclusion

The focus of this chapter was to provide a highly efficient high-order numerical method for numerically solving the two-dimensional TFCDE. A notable aspect of this problem was the utilization of the Caputo time-fractional derivative, which led to an initial weak singularity at $t = 0$. The core foundation of the proposed scheme centered around the utilization of two key components: the adoption of the L2-1_σ approximation formula for the Caputo time-fractional derivative implemented on a fitted mesh and a high-order compact finite difference approximation for the space derivatives on a uniform mesh. Moreover, to solve the resulting system, a two-step ADI (Alternating Direction Implicit) approach is employed. In addition, a rigorous theoretical analysis has been undertaken, thoroughly assessing the stability and convergence of the proposed scheme. Our findings demonstrated that the method exhibits unconditional stability for every $\alpha \in (0, 1)$, accompanied by uniform convergence with an order of $\mathcal{O}\left(N_t^{-\min\{3-\alpha,\theta\alpha,1+2\alpha,2+\alpha\}} + h_x^4 + h_y^4\right)$. Through extensive numerical experiments conducted on two test problems featuring a non-smooth solution, we have observed that our proposed scheme surpassed other existing schemes in terms of higher-order convergence and numerical results validated to our theoretical analysis. Also, it became apparent that proposed numerical algorithm on a fitted mesh outperforms the method on a uniform mesh.